

DAMAGE MECHANICS-BASED MODEL FOR THE DEFORMATION
RESPONSE AND FAILURE OF COMPOSITE HONEYCOMB CORE
STRUCTURE

MUHAMMAD SALMAN KHAN

UNIVERSITI TEKNOLOGI MALAYSIA

DAMAGE MECHANICS-BASED MODEL FOR THE DEFORMATION
RESPONSE AND FAILURE OF COMPOSITE HONEYCOMB CORE
STRUCTURE

MUHAMMAD SALMAN KHAN

A thesis submitted in fulfilment of the
requirements for the award of the degree of
Doctor of Philosophy

School of Mechanical Engineering
Faculty of Engineering
Universiti Teknologi Malaysia

OCTOBER 2021

ACKNOWLEDGEMENT

First and foremost, I want to thank Allah Almighty, the Most Gracious, the Most Merciful, the Most Bountiful, Who gave me courage and patience to accomplish this research work. Without His blessings and mercy, this would not have come to reality.

I would like to express my gratitude for the guidance and technical support from my supervisor, Prof. Dr Mohd. Nasir Bin Tamin, on his continuous encouragement and valuable comments throughout the research work. I am fortunate to be one of his graduate students. His experience and creativity gave me great knowledge for carving my future career.

I want to acknowledge my colleagues at the Computational Solid Mechanics Laboratory (CSMLab) who have been helpful and friendly, never fail to make the lab a pleasant place to work. Many thanks to Dr Muhammad Adil Khattak for sharing technical skills and knowledge. His guidance and support helped me in getting many publications through collaborative research work. I am also indebted to the National University of Science and Technology (NUST) for funding my doctoral degree.

Finally, but not the least, my sincere thanks from the depth of the heart to my family for giving unlimited support and patience. I appreciate the sacrifice of my father, my late mother and sisters in helping me financially and morally to finish my study.

ABSTRACT

The development of phenolic resin-based *Nomex* hexagonal Honeycomb (HC) structures is of great interest in recent years for low density, low in-plane, and high out-of-plane stiffness values achieving stable deformations over a wide range of structural geometries. Nonlinear elastic behavior covering the large geometric deformation is the critical issue in analyzing the mechanical response and failure of the cellular core structure. A useful approach for modeling such complex behavior is to replace the cellular structure with an equivalent homogenous material that represents identical mechanical behavior for the respective HC structure. This research aims to develop a Representative Cell (RC) model for the *Nomex* HC core and subsequently replace that with a homogenous orthotropic material of equivalent elastic properties utilizing the homogenization approach. A series of experimental testing was performed on the HC core to identify the nine elastic constants comprising both in-plane and out-of-plane properties. The single unit cell structure is selected based on the parametric analysis through compression testing of the hexagonal HC cores with different cell geometries to compare the compression strength and energy absorption capacity. The selected cell geometry with 3.2 mm cell size, 12.7 mm height, and 0.05 mm paper thickness is used to develop a meso-scale solid element RC model to show the mechanical deformation under out-of-plane compression and shear loading. The constituent orthotropic material model along with Hashin damage parameters was used as input for phenolic resin-based *Nomex* paper in ABAQUS finite element analysis software. A direct homogenization method was employed to develop a homogenized equivalent homogenized honeycomb core (EHC) model. The model is examined to assess the predicted equivalent elastic properties against the stiffness matrix obtained by experimentation. The comparative analysis for the *Nomex* HC structural characterization showed that the geometric configurations, specifically the relative density and cell aspect ratio (height/cell size), greatly influence the mechanical properties. The optimum values obtained for the elastic moduli and compression strength were 126.5 MPa and 4.01 MPa, respectively, with a relative density of 0.056 and a cell aspect ratio of 3.96. Compared with the experimental testing results from compression loading, the developed damage mechanics-based RC model demonstrated less than a 2% difference in the collapse/compression strength and elastic moduli of the selected HC core. The EHC model was verified using a three-point bend loading condition. The predicted flexural strength compared to the measured data had a minimal variation of only 4%. The developed EHC model can be effectively used to predict the mechanics of deformation and failure properties in the complex sandwich structures. The damage mechanics-based methodology presented in this research work could be implemented for complex structural parts in the aerospace and transport industry for reducing the need of extensive experimental testing eventually minimizing the developmental cost and time.

ABSTRAK

Pembangunan struktur indung madu heksagon *Nomex* berasaskan resin fenolik mula mendapat perhatian dalam beberapa tahun kebelakangan ini kerana nilai ketumpatannya yang rendah, sifat kekukuhan yang rendah di dalam satah dan tinggi di luar satah membolehkan deformasi yang stabil dalam pelbagai struktur geometri. Ciri-ciri elastik bukan lurus yang merangkumi deformasi geometri besar adalah masalah penting dalam menganalisa tindak balas mekanikal dan kegagalan struktur teras selular. Pendekatan yang berguna bagi pemodelan ciri-ciri kompleks seperti itu adalah dengan mengganti struktur selular dengan bahan homogen yang setara yang mewakili ciri-ciri mekanikal yang sama untuk struktur HC masing-masing. Objektif penyelidikan ini adalah untuk membangunkan model Cell Perwakilan (RC) untuk teras *Nomex* HC dan seterusnya menggantinya dengan bahan ortotropik homogen yang mempunyai ciri-ciri elastik yang setara dengan menggunakan pendekatan homogenisasi. Siri ujian eksperimen dilakukan pada teras HC untuk mengenal pasti sembilan pemalar elastik yang terdiri daripada sifat dalam dan luar satah. Struktur sel unit tunggal dipilih berdasarkan analisis parametrik melalui ujian mampatan teras HC heksagon dengan geometri sel yang berbeza untuk membandingkan kekuatan mampatan dan kapasiti penyerapan tenaga. Geometri sel yang dipilih dengan ukuran sel 3.2 mm, tinggi 12.7 mm dan ketebalan kertas 0.05 mm telah digunakan untuk membangunkan model RC elemen pepejal berskala meso untuk menunjukkan deformasi mekanikal di bawah pemampatan luar satah dan beban ricih. Model bahan berunsur ortotropik bersama dengan parameter kerosakan Hashin digunakan sebagai input untuk kertas *Nomex* berasaskan resin fenolik dalam perisian ABAQUS. Kaedah homogenisasi langsung digunakan untuk membangunkan model teras HC yang homogen. Model tersebut diperiksa untuk menilai sifat elastik setara yang dijangkakan terhadap (EHC) matriks kekukuhan yang diperolehi melalui eksperimen. Analisa perbandingan untuk pencirian struktur *Nomex* HC menunjukkan bahawa konfigurasi geometri khususnya kepadatan relatif dan nisbah aspek sel (ketinggian/saiz sel) sangat mempengaruhi ciri-ciri mekanikalnya. Nilai optimum yang diperolehi untuk moduli elastik dan kekuatan mampatan masing-masing adalah 126.5 MPa dan 4.01 MPa, dengan ketumpatan relatif 0.056 dan nisbah aspek sel 3.96. Model RC berasaskan mekanik kerosakan yang telah dibangunkan tersebut, apabila dibandingkan dengan hasil ujian eksperimen dari beban mampatan menunjukkan perbezaan kurang dari 2% dalam kekuatan keruntuhan/mampatan dan moduli elastik teras HC yang dipilih. Model teras HC homogen yang setara telah disahkan menggunakan kaedah beban lentur tiga titik. Kekuatan lenturan yang dijangkakan berbanding dengan data yang diukur mempunyai variasi yang sangat kecil iaitu hanya 4%. Model teras EHC yang telah dibangunkan dapat digunakan dengan berkesan untuk meramalkan mekanisma sifat ubah bentuk dan kegagalan dalam struktur himpitan yang kompleks. Metodologi berasaskan mekanik kerosakan yang disajikan dalam karya penyelidikan semasa dapat dilaksanakan untuk komponen struktur yang kompleks di industri aeroangkasa dan pengangkutan untuk mengurangkan keperluan pengujian eksperimen yang luas akhirnya meminimumkan kos dan waktu pembangunan.

TABLE OF CONTENTS

	TITLE	PAGE
	DECLARATION	iii
	DEDICATION	iv
	ACKNOWLEDGEMENT	v
	ABSTRACT	vi
	ABSTRAK	vii
	TABLE OF CONTENTS	viii
	LIST OF TABLES	xiii
	LIST OF FIGURES	xiv
	LIST OF ABBREVIATIONS	xxi
	LIST OF SYMBOLS	xxii
	LIST OF APPENDICES	xxvi
CHAPTER 1	INTRODUCTION	1
	1.1 Honeycomb Core Structure	1
	1.2 Research Background	3
	1.3 Statement of Research Problem	6
	1.4 Research Objectives	7
	1.5 Scope of the study	7
	1.6 Significance of the Study	10
	1.7 Thesis Layout	10
CHAPTER 2	LITERATURE REVIEW	15
	2.1 Introduction	15
	2.2 HC Core as Part of the Sandwich Structure	15
	2.3 Geometry of Cellular HC Cores	17
	2.4 Materials Used for HC Cores	19
	2.4.1 Aluminum	20
	2.4.2 <i>Nomex</i> Paper	21

2.5	Mechanical Behavior and Structure Properties of HC Core	23
2.5.1	Deformation Response and Failure Mechanisms	23
2.5.2	Effects of Geometric Parameters	28
2.6	Finite Element Modeling for HC Core Structure	30
2.6.1	Representative Cell Models	32
2.6.2	Constitutive Material Models	34
2.6.2.1	Single Layer Isotropic	34
2.6.2.2	Single Layer Orthotropic	35
2.6.2.3	Multi-Layer Resin Coating	37
2.7	Damage Mechanics-Based Analysis of HC Core Structure	41
2.7.1	Failure Criteria for Composite Materials	43
2.7.1.1	Hashin Damage Model Criteria	46
2.8	Homogenization Concepts for HC Core Structure	49
2.8.1	Out-of-Plane Elastic Constants	53
2.8.2	In-Plane Elastic Constants	55
2.8.3	Strain Energy-based Homogenization Approach	57
2.9	Summary	58
CHAPTER 3	RESEARCH METHODOLOGY	61
3.1	Introduction	61
3.2	Research Framework	61
3.3	Extraction of <i>Nomex</i> Paper Material Properties	64
3.4	HC Core Cellular Configuration and Geometric Parameters	66
3.5	Mechanical Test Procedures for HC Core	67
3.5.1	Flatwise Tension Test	68
3.5.2	Flatwise Compression Test	69
3.5.3	Shear Test	70
3.5.4	Edgewise Tension Test	73
3.5.5	Three-Point Bend Test of Sandwich HC Panel	74
3.6	Damage-Based Representative Cell Model for HC Core	76
3.6.1	Representative Unit Cell Models	77
3.6.2	Boundary Conditions and Load Cases	78

3.6.3	Material Properties and Damage Model Parameters	79
3.6.4	Mesh Convergence Analysis	81
3.6.5	Element Type Selection	82
3.6.6	Representative Cell FE Model Validation	84
3.7	Development of Equivalent Homogenized HC Core Model	84
3.7.1	Representative Structures	85
3.7.2	Element Type, Mesh Size and Boundary Conditions for EHC Models	87
3.7.3	Extraction of Structural Properties	89
3.7.3.1	Elastic Constants for Stiffness Matrix	90
3.7.3.2	Structural Damage Model Parameters	90
3.7.4	EHC Model Verification	91
3.8	Summary	93
CHAPTER 4	MECHANICAL PROPERTIES AND BEHAVIOR OF HONEYCOMB CORE STRUCTURE	95
4.1	Introduction	95
4.2	Tensile Properties of Phenolic Resin-Based <i>Nomex</i> Paper	95
4.2.1	Elastic Constants	96
4.2.2	Damage Model Parameters	97
4.3	Deformation Responses and Failure Mechanism of HC Core Structures	98
4.3.1	Out-of-Plane Tension	99
4.3.2	Out-of-Plane Compression	101
4.3.3	Out-of-Plane Shear	104
4.3.4	In-Plane Tension	106
4.3.5	In-Plane Shear	108
4.4	Flexure Response of HC Sandwich Panel Under Three-Point Bending	110
4.5	Summary	111
CHAPTER 5	EFFECTS OF CELL ASPECT RATIO AND RELATIVE DENSITY ON THE DEFORMATION RESPONSE AND FAILURE OF HONEYCOMB CORE	113
5.1	Introduction	113

5.2	Effects of Design Parameters on the Structural Properties	113
5.2.1	Relative Density	115
5.2.2	Cell Height	116
5.2.3	Hexagonal Cell Size	118
5.3	Comparative Analysis of Mechanical Properties	120
5.3.1	Effects on the Elastic Modulus	120
5.3.2	Dissipated Energy Density Comparison	121
5.3.3	Phenomenological Model for the Compressive Strength of HC Core	122
5.4	Summary	130
CHAPTER 6	REPRESENTATIVE CELL ANALYSIS FOR DAMAGE-BASED FAILURE MODEL OF HONEYCOMB CORE UNDER OUT-OF-PLANE LOADINGS	133
6.1	Introduction	133
6.2	Failure under the Out-of-Plane Tension	133
6.3	Out-of-Plane Compression Responses	139
6.4	Out-of-Plane Shear Failure	146
6.4.1	In Transverse Orientation	147
6.4.2	In Ribbon Orientation	153
6.5	Comparative Analysis of Out-of-Plane Mechanical Properties	158
6.6	Summary	160
CHAPTER 7	DEVELOPMENT OF EQUIVALENT HOMOGENIZED HONEYCOMB CORE MODEL	163
7.1	Introduction	163
7.2	Equivalent Homogenized HC Core (EHC) Model	163
7.2.1	Structural Properties for EHC Model	164
7.2.2	Elastic Constants and its Comparison with Theoretical Models	165
7.2.3	Damage Model Parameters	166
7.3	Damage Mechanics-Based Equivalent HC Core Model Results	167
7.3.1	Multi-Cell Equivalent Model	168
7.3.2	Single-Cell Equivalent Model	172

7.4	Verification of EHC Model	178
	7.4.1 Sandwich HC Panel FE Model Failure Analysis	180
7.5	Summary	184
CHAPTER 8	CONCLUSIONS AND RECOMMENDATIONS	185
8.1	Conclusions	185
8.2	Contribution of the Work	187
8.3	Recommendations for Future Work	188
	REFERENCES	189
	LIST OF PUBLICATIONS	208

LIST OF TABLES

TABLE NO.	TITLE	PAGE
Table 2.1	Hexagonal HC core geometric parameters [67-69]	19
Table 2.2	Review summary of material models used for FE analysis of <i>Nomex</i> HC core structure	39
Table 3.1	HC cell configuration	67
Table 3.2	Strength properties of phenolic resin impregnated <i>Nomex</i> paper	80
Table 3.3	Comparison of the computational parameters used for the FE Single-Cell model under tension with conventional and continuum shell elements.	84
Table 3.4	EHC FE model parameters	89
Table 3.5	Extraction of damage initiation parameters from measured data and numerical analysis of real HC core structure	91
Table 3.6	Element types and distribution for the three-point bend numerical model	93
Table 4.1	Properties of phenolic resin impregnated <i>Nomex</i> paper	97
Table 4.2	Constitutive damage model parameters of polymeric <i>Nomex</i> paper	98
Table 4.3	Mechanical properties of <i>Nomex</i> HC* core structure in different load orientations	112
Table 5.1	Specifications of the HC core specimens	114
Table 6.1	Comparison in mechanical properties (compression loading)	141
Table 6.2	Mechanical properties for all FE models compared to the measured data	159
Table 7.1	Comparison of out of plane elastic constants for <i>Nomex</i> HC core	166
Table 7.2	Structural properties for EHC model	167
Table 7.3	Comparison of EHC model mechanical properties with measured data	180

LIST OF FIGURES

FIGURE NO.	TITLE	PAGE
Figure 1.1	Honeycomb (HC) core application in sandwich panel	2
Figure 1.2	(a) HC application in airframe structure (Airbus A380), (b) wooden surfboard and (c) Non-pneumatic tire with HC spokes [21]	2
Figure 2.1	HC core cellular configurations [1]	18
Figure 2.2	Hexagonal HC core cellular configuration [69]	18
Figure 2.3	Paper-based hexagonal HC core manufacturing process [1, 29]	23
Figure 2.4	Failure modes of HC core sandwich panel under flexure load [109]	25
Figure 2.5	Tensile and compressive load-displacement curves of the resin-impregnated fiber-reinforced paper HC core [24-25, 29].	26
Figure 2.6	Out-of-plane compression load-displacement responses with different cell size for HC cores (a) aluminum, (b) <i>Nomex</i> [27]	27
Figure 2.7	Classification of multiscale methods for numerical modeling of HC core structure.	31
Figure 2.8	Representative cell (RC) models for hexagonal HC core [29].	33
Figure 2.9	Material modeling approaches for phenolic resin-based <i>Nomex</i> HC core structure [27, 29, 36, 50]	34
Figure 2.10	Stress-strain relationship for different material models; (a) Linear elastic isotropic material [25] and (b) Linear elastic orthotropic material [29]	35
Figure 2.11	Phenolic resin impregnation in the <i>Nomex</i> HC core specimen [94]	37
Figure 2.12	Mechanics of materials and analysis classification (based on [134, 135])	42
Figure 2.13	Longitudinal and transverse orientation in a composite lamina [40]	44
Figure 2.14	Bi-linear softening laws for composite lamina [40]	48

Figure 2.15	Bi-linear traction-separation curve for Mode I loading of a composite lamina [135].	49
Figure 2.16	Hexagonal HC core; (a) RVE single-cell and (b) Equivalent homogenized volume [147]	51
Figure 2.17	Illustration of the out-of-plane elastic constants for the HC core [70]	53
Figure 3.1	Flowchart of the research activities	62
Figure 3.2	Phenolic resin-based <i>Nomex</i> paper (a) tension test setup, (b) geometry of the specimen.	65
Figure 3.3	Hexagonal HC core	66
Figure 3.4	(a) The assembly of the HC sandwich specimen in the flatwise tensile test jig, and (b) the HC sandwich specimen with the loading blocks.	68
Figure 3.5	HC core flatwise compression test setup	70
Figure 3.6	(a) HC core out-of-plane shear loading jig, (b) ribbon orientation (G_{13}) and (c) transverse orientation (G_{23}).	71
Figure 3.7	HC core in-plane shear test setup	72
Figure 3.8	Fabricated jigs for hexagonal HC core in-plane tension loading	73
Figure 3.9	HC core test setup for in-plane tension loading, (a) Ribbon orientation (X_1) and (b) Transverse orientation (X_2).	74
Figure 3.10	Schematic diagram and sandwich specimen dimensions,	76
Figure 3.11	Sandwich HC panel three-point bend test (3PBT) setup.	76
Figure 3.12	(a) Single-Cell and (b), (c) Multi-cell models for the out-of-plane tension and compression, and (d), (e) 6-cell model for the out-of-plane shear in the transverse and ribbon direction, respectively.	78
Figure 3.13	(a) Cell wall thickness of the HC core at different magnification and (b) distribution of the wall thickness of the HC cell.	80
Figure 3.14	Mesh convergence analysis outcomes based on the out-of-plane compressive load case with the Single-Cell model.	82
Figure 3.15	Conventional and continuum shell element description	83
Figure 3.16	Comparison of the FE-calculated responses of the Single-Cell model with the measured curve for the tensile load case.	83
Figure 3.17	Multi-Cell EHC model	86

Figure 3.18	Single-Cell (RC-1) replaced by Single-Cell EHC model with same geometric dimensions.	87
Figure 3.19	EHC models with boundary conditions (a) Single-Cell (mesh size: 0.2) and (b) Multi-Cell (mesh size: 1)	88
Figure 3.20	Mesh convergence for Multi-Cell EHC model	88
Figure 3.21	Three-point bend FE model geometry and boundary conditions	92
Figure 4.1	Phenolic resin-based <i>Nomex</i> paper tension test graphs	97
Figure 4.2	Tensile load-displacement curves of the HC core with CFRP face sheets.	100
Figure 4.3	HC Sandwich Specimen (a) before the flatwise tension test and (b) at the end of the test.	101
Figure 4.4	Load-displacement curves of the HC core under flatwise compressive loading	102
Figure 4.5	The geometry (side view) of the HC core specimen at the various stages of the flatwise compression test. Refer to Figure 4.4 for the corresponding load and displacement values.	103
Figure 4.6	(a) The as-received hexagonal HC core, and (b) after the flatwise compression test.	103
Figure 4.7	Out-of-plane shear load-displacement curves of the HC core with the transverse and ribbon orientation.	104
Figure 4.8	Deformed and fracture features of the HC core with transverse orientation (a, b and c) and ribbon orientation (d, e and f) under the out-of-plane shear loading. The corresponding loading stage is as indicated in Figure 4.7.	105
Figure 4.9	In-plane tension load-displacement curves of the HC core. (a) Transverse orientation, X_2 , (b) Ribbon orientation, X_1	107
Figure 4.10	Fracture features of the in-plane tensile test specimens of the HC core with (a) Transverse orientation, X_2 , (b) Ribbon orientation, X_1	108
Figure 4.11	In-plane shear load-displacement curves of the HC core.	109
Figure 4.12	Fracture of cell walls during in-plane shear loading of HC core	110
Figure 4.13	(a) Flexure load-displacement response and (b) sandwich HC core panel testing	111
Figure 5.1	Stress-strain curves of the HC cores with different relative densities (Cell aspect ratio, $H/c = 3.96$).	115

Figure 5.2	Failure features of the HC core specimens at a different relative density of (a) 0.056 (B2) and (b) 0.112 (C2). The cell height, $H = 12.7$ mm.	116
Figure 5.3	Stress-strain curves of the HC cores with different cell aspect ratio, H/c ($c = 3.2$ mm, $\rho^*/\rho_s = 0.056$)	117
Figure 5.4	Failure features of the HC core specimens with different cell heights of (a) 8 mm (specimen B1) and (b) 18 mm (specimen B3).	118
Figure 5.5	Comparison of the stress-strain curves for different cell size; Specimen A2 ($c = 4.8$ mm, $\rho^*/\rho_s = 0.028$) and specimen B2 ($c = 3.2$ mm, $\rho^*/\rho_s = 0.056$).	119
Figure 5.6	Before and after compression fractographs of specimen A2 ($c = 4.8$ mm, $\rho^*/\rho_s = 0.028$)	119
Figure 5.7	Variations of elastic modulus with the cell aspect ratio and relative density of the HC core.	121
Figure 5.8	Variation of the dissipation energy density with the cell aspect ratio of the <i>Nomex</i> HC cores	122
Figure 5.9	The variation of compressive strengths with the relative density of the <i>Nomex</i> HC cores. The filled symbols represent data from the current study	123
Figure 5.10	Variations of compressive strengths with cell aspect ratio and relative density of HC core.	124
Figure 5.11	$\ln\sigma c$ versus $1H/c$, where ($H/c \leq 3.96$). ($H/c = 3.96$ is considered as starting point).	125
Figure 5.12	Compressive Strength, σc vs $1H/c$	127
Figure 5.13	$\ln\sigma c$ versus $1H/c$, where ($H/c > 3.96$)	127
Figure 5.14	Illustration of the phenomenological model in Eqn. (5.15) and (5.16).	129
Figure 5.15	Graphical illustration of the effects of relative density and cell aspect ratio on the compressive strength of HC core: (a) $H/c > 3.96$, $r^2 = 0.9768$ and (b) $H/c \leq 3.96$, $r^2 = 0.9752$.	130
Figure 6.1	Comparison of FE-calculated and measured tensile responses of the HC core	134
Figure 6.2	(a) Damage initiation and evolution to separation, and (b) the corresponding stresses at the critical material point in the cell wall of the HC core.	135

Figure 6.3	(a) Damage evolution at $dpmt = 1$ and (b) max principal stress contours of Single-cell FE model with increasing displacement.	136
Figure 6.4	(a) Location of the fractured plane along the cell height and (b) fractured surface of the polymer hexagonal HC core specimen following the out-of-plane tensile loading.	137
Figure 6.5	(a) Damage evolution ($dpmt = 1$) and (b) Maximum principal stress contours of 4-Cell FE model with increasing displacement.	138
Figure 6.6	The measured compressive load-displacement responses of the HC core panel with different sizes (core thickness, $H = 12.7$ mm).	139
Figure 6.7	Comparison of the measured and the FE-calculated compressive load-displacement responses for the different FE models of the HC core.	140
Figure 6.8	(a) Evolution of the matrix damage variable to the onset of damage and subsequent damage evolution, (b) contour of the damage at the start of the global buckling of the HC cell.	143
Figure 6.9	Contours of the minimum principal stress in the single-cell and 4-cell HC core model. Values plotted correspond to the onset of localized buckling of the critical material points in the cell wall	144
Figure 6.10	Distribution of minimum principal stress in the cell wall material (Top) and deformation (Bottom) during the out-of-plane compression test of the one-cell specimen. (a) matrix damage, $dpmc = 0$, following damage initiation, (b) $dpmc = 0.75$, showing wrinkling of the unconstrained cell walls, and (c) $dpmc = 1.0$, with the occurrence of the first fold.	145
Figure 6.11	Total displacement fields following the densification of the single-cell FE model.	146
Figure 6.12	Comparison of the measured and FE-calculated out-of-plane shear stress-strain responses of the HC core	147
Figure 6.13	(a) Failed HC core specimen under the out-of-plane shear in the transverse direction, illustrating the critical shear plane, and (b) the corresponding FE-calculated shear stress in the HC core model.	148
Figure 6.14	Similar variation of the shear stress τ_{23} and the maximum principal stress along the shearing plane (Path 2), indicating the pure shear test condition.	148

Figure 6.15	(a) Minimum principal stress, and (b) the matrix compressive damage contour, corresponding to the applied shear displacement of 0.33 mm.	149
Figure 6.16	(a) Shear load-displacement response in the transverse direction, (b) Evolution of damage initiation and subsequent damage for the material point marked C in Figure 6.15 (b), and (c) Evolution of stresses of the HC core	150
Figure 6.17	(a) Evolution of damage and stresses for the material point marked as Node D, (b) Matrix tension damage contour and (c) Maximum principal stress distribution, corresponding to the applied shear displacement of 0.33 mm in Figure 6.16(a).	152
Figure 6.18	Damage evolution contours at 0.59mm displacement (see Figure 6.16 and Figure 6.17 (a)) in transverse orientation shear load for (a) Matrix compression and (b) Matrix tension.	153
Figure 6.19	(a) Failed HC core specimen under the out-of-plane shear in ribbon direction, illustrating the critical shear plane, and (b) the corresponding FE-calculated shear stress in the HC core model.	154
Figure 6.20	Variation of the shear stress, τ_{13} and the maximum principal stress along (a) Path 3 (shearing plane), and (b) Path 4 of the HC core model.	154
Figure 6.21	(a) Maximum principal stress, and (b) the matrix tension damage initiation contour, corresponding to the applied shear displacement of 0.33 mm.	155
Figure 6.22	(a) Shear load-displacement response in Ribbon direction, (b) Evolution of damage initiation and subsequent damage for the material point marked E in Figure 6.21 (b), and (c) Evolution of stresses during the shear test	156
Figure 6.23	(a) Evolution of damage and stresses for the material point marked as Node F, (b) Matrix compression damage contour and (c) Minimum principal stress distribution at the applied shear displacement of 0.45 mm in Figure 6.22 (a).	157
Figure 6.24	(a) Matrix tension damage evolution at $dpmt = 1$ and (b) Maximum principal stress corresponding to the displacement of 0.6 mm (see Figure 6.22 (a)) in Shear Load (Ribbon Orientation).	158
Figure 6.25	Comparison of relative wall-clock time taken by the different cell models for the out-of-plane load cases.	160

Figure 7.1	Out-of-Plane Compression load-displacement plots for the Multi-Cell HC Core FE models and measured data	169
Figure 7.2	Multi-Cell EHC model damage initiation and Stress plots. Contours are shown in (b) and (c) for peak load at 0.37 mm displacement.	170
Figure 7.3	Contours at 1 mm displacement for (a) Minimum principal stress and (b) Matrix compression damage evolution, $dpmc = 0.95$	171
Figure 7.4	Total displacement in Multi-Cell EHC model following the crushing due to compression loading.	171
Figure 7.5	Out-of-Plane compression load-displacement plots for the Single-Cell HC Core FE models and measured response.	173
Figure 7.6	Single-Cell EHC model response under out-of-plane compression (a) Damage and stresses plots at Node K. Contours at 0.33 mm displacement for (b) Damage initiation and (c) Minimum principal stress.	174
Figure 7.7	Matrix compression damage evolution ($dpmc=1$) at 0.5 mm displacement, (a) Single-cell EHC Model, (b) Single-Cell (RC-1) Model	175
Figure 7.8	Deformed and undeformed geometry of the Single-Cell EHC model	176
Figure 7.9	Comparison of compression load-displacement graphs of EHC FE models and the measured data, including the crushing zone (plateau stress).	177
Figure 7.10	EHC models responses with the increase in the number of cells. (The dashed lines represent the measured value)	178
Figure 7.11	Three-point bend loading response of sandwich HC structure	179
Figure 7.12	Sandwich HC panel in three-point bend loading; (a) Maximum principal stress in face-sheets, (b) Minimum principal stress in EHC and (c) Deformed specimen after experimentation	181
Figure 7.13	Damage initiation graphs and stress plots for matrix region in the equivalent HC core of the sandwich panel. The nodes are identified in Figure 7.14.	182
Figure 7.14	Damage initiation contours in EHC model; (a) Matrix compression and (b) Matrix tension.	183
Figure 7.15	EHC model deformation in matrix tension region (a) Damage evolution ($dpmt = 1$), (b) Shear stress field.	183

LIST OF ABBREVIATIONS

HC	-	Honeycomb
GFRP	-	Glass fiber reinforced polymer
CFRP	-	Carbon fiber reinforced polymer
FE	-	Finite element
RVE	-	Representative volume element
RC	-	Representative cell
3D	-	Three-Dimensional
ABS	-	Acrylonitrile butadiene styrene
PLA	-	Polylactic acid
Al-Li	-	Aluminum Lithium
HOBE	-	Honeycomb before expansion
S4R	-	4 node shell element with reduced integration
C3D8R	-	Continuum 3 D Solid element with reduced integration
LTC	-	Lee and Tsotsis criteria
SVS	-	Shell–volume–shell
3PBT	-	Three-point bend test
ASTM	-	American Standard for Testing of Materials
SC8R	-	Continuum 8 node shell element
DOF	-	Degree of freedom
CPU	-	Central processing unit
EH	-	Equivalent homogenous
DED	-	Dissipation energy density
EHC	-	Equivalent homogeneous honeycomb core
MT	-	Matrix Tension
MC	-	Matrix Compression

LIST OF SYMBOLS

l	-	Cell wall length
c	-	Cell size
t	-	Paper thickness
θ	-	Core angle
L	-	Panel length
W	-	Panel width
H	-	Core height
ρ^*	-	Density of the core
ρ_s	-	Cell wall material density
t	-	Cell wall thickness
E_{iso}	-	Young's modulus for Isotropic material
σ_{yield}	-	Yield strength for isotropic material
ν_{iso}	-	Poisson's ratio for isotropic material
E_1	-	Elastic Modulus in the longitudinal direction
E_2	-	Elastic Modulus in the transverse direction
E_3	-	Elastic Modulus in out-of-plane orientation
$\sigma_{1,T}$	-	Tensile strength in the longitudinal direction
$\sigma_{2,T}$	-	Tensile strength in the transverse direction
$\sigma_{1,C}$	-	Compression strength in the longitudinal direction
$\sigma_{2,C}$	-	Compression strength in the transverse direction
σ_{11}	-	Stress in the fiber direction
σ_{22}	-	Stress in the transverse direction
τ_{12}	-	Shear stress
ϵ_{11}	-	Strain in the fiber direction
ϵ_{22}	-	Strain in the transverse direction
γ_{12}	-	Shear strain
X	-	Longitudinal strength
Y	-	Transverse strength
S	-	Shear strength
X_E	-	Maximum allowable strain in the longitudinal direction

Y_E	-	Maximum allowable strain in the transverse direction
S_E	-	Maximum allowable shear strain
X^T	-	Longitudinal tensile strength
Y^T	-	Transverse tensile strength
S^T	-	Longitudinal shear strength
X^C	-	Longitudinal compressive strength
Y^C	-	Transverse compressive strength
S^C	-	Transverse shear strength
d_f^t	-	Damage initiation variable for fiber tension
d_f^c	-	Damage initiation variable for fiber compression
d_m^t	-	Damage initiation variable for matrix tension
d_m^c	-	Damage initiation variable for matrix compression
d_p^{mt}	-	Damage evolution variable for matrix tension
d_p^{mc}	-	Damage evolution variable for matrix compression
d_p^{ft}	-	Damage evolution variable for fiber tension
d_p^{fc}	-	Damage evolution variable for fiber compression
K	-	Stiffness
N	-	Mode I strength
δ_N^0	-	Relative displacement at the damage onset
δ_N^f	-	relative displacement at the fracture
G_{1C}	-	Mode I fracture energy
E_{11}	-	Elastic modulus in the ribbon direction
E_{22}	-	Elastic modulus in the transverse direction
E_{33}	-	Elastic modulus in the thickness direction
G_{12}	-	In-plane shear modulus
G_{13}	-	Out-of-plane shear modulus
G_{23}	-	Out-of-plane shear modulus in the thickness direction
ν_{12}	-	In-plane Poisson's ratio
ν_{13}	-	In-plane Poisson's ratio
ν_{23}	-	Out-of-plane Poisson's ratio in the thickness direction
σ_{33}	-	Stress in the out-of-plane loading
ε_{33}	-	Strain in the out-of-plane loading

ε_{11}	-	Strain in the longitudinal (fiber) direction
ε_{22}	-	Strain in the transverse (matrix) direction
τ_{13}	-	Shear strength in the ribbon direction
γ_{13}	-	Shear strain in the ribbon direction
τ_{23}	-	Shear strength in the transverse direction
γ_{23}	-	Shear strain in the transverse direction
E_s	-	Elastic modulus of the material
G_s	-	Shear modulus of the material
ν_s	-	Poisson's ratio of material
V	-	Volume of the representative volume element
$\underline{\underline{\sigma}}(\underline{x})$	-	Stress at a material point (\underline{x})
$\underline{\underline{\epsilon}}(\underline{x})$	-	Strain at a material point (\underline{x})
$\underline{\underline{\Sigma}}$	-	Equivalent stress for macro-scale homogeneous material
$\underline{\underline{E}}$	-	Equivalent strain for macro-scale homogeneous material
F_z^{fcu}	-	Ultimate flatwise compressive strength (MPa)
P_{max}	-	Ultimate force before failure
A	-	Cross-sectional area
τ	-	Core shear stress
P	-	Applied load
γ	-	Core shear strain
u	-	Displacement between the loading plates
F_s^{ult}	-	Core ultimate shear strength
d	-	Sandwich thickness
b	-	Sandwich width
δ_{eq}^0	-	Equivalent displacement at the onset of damage
δ_{eq}	-	Equivalent displacement at any step
δ_{eq}^f	-	Equivalent displacement at the fracture
G_{XT}	-	Longitudinal tensile fracture energy
G_{XC}	-	Longitudinal compressive fracture energy
G_{YT}	-	Transverse tensile fracture energy
G_{YC}	-	Transverse compressive fracture energy

$\sigma_{min.p}$	-	Minimum principal stress
∞	-	Infinity
G_C	-	Equivalent dissipation energy
E_T	-	Tensile strength of the HC core
E_C	-	Compression strength of the HC core
σ_T	-	Tensile strength of HC core
σ_C	-	Compression strength of HC core
X_1	-	Ribbon direction
X_2	-	Transverse direction
n	-	Exponent for relative density
α	-	Exponent for cell aspect ratio
C	-	Constant
α_{avg}	-	Average of the exponent for cell aspect ratio
U_3	-	Displacement in out-of-plane direction

LIST OF APPENDICES

APPENDIX	TITLE	PAGE
Appendix A	Hexagonal Jig Designs for In-Plane Tensile Test	203
Appendix B	Damage at Different Paths in Single-Cell EHC Model	206
Appendix C	Compression Load/Displacement Plots of EHC Models	207

CHAPTER 1

INTRODUCTION

1.1 Honeycomb Core Structure

Honeycomb (HC) sandwich panels have found numerous engineering applications in the aerospace and transportation industry. This is primarily due to their high strength-to-weight ratio, high structural stiffness, and improved resistance to the harsh operating environment [1]. Also, these lightweight structures offer an excellent capability to withstand through-thickness compression. The HC sandwich panel is constructed by laminating a HC cellular core structure's outer surfaces with thin and stiff face sheets. The face sheets are glued together with the thick core using adhesive films, resulting in a three-layered sandwich panel, as shown in Figure 1.1. It is designed such that the HC core not only maintains the distance between the face sheets and improves the flexural stiffness but also carries the normal compression and shear loads [2, 3]. The selection of face sheet material and its thickness, along with the material and geometry of the core, offers several choices for designers allowing tailor-made structural properties, including not only mechanical but also acoustic and thermodynamic aspects. The common HC cores with square or hexagonal cells [4] are fabricated from metallic alloys such as aluminum [5-7], and polymers including Kevlar or Aramid resin-impregnated papers [8-11]. The face sheets are typically made of aluminum [12, 13], glass fiber-reinforced polymer (GFRP) [14, 15], or carbon fiber-reinforced polymer (CFRP) composite laminates [3, 16].

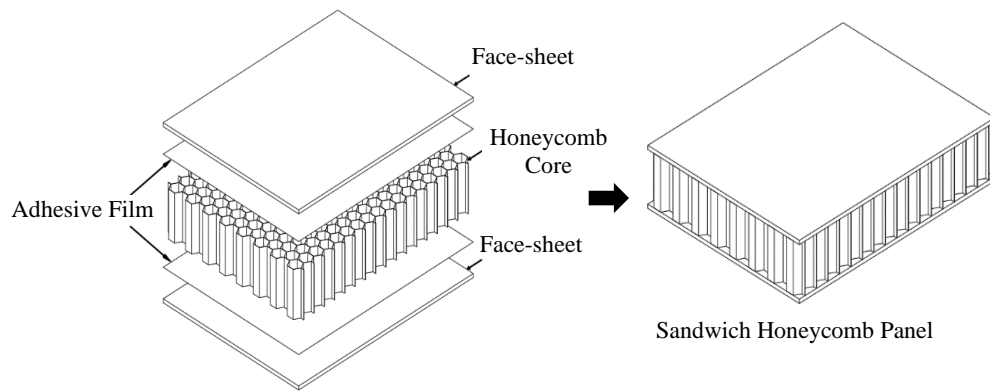


Figure 1.1 Honeycomb (HC) core application in sandwich panel

The extensive application of polymeric composite sandwich panels in the aerospace industry has continuously increased over the last decades. Modern aircraft design like the Airbus A380 was among the first commercial airplane using 25 % of the composite structures, including the sandwich panels in the aircraft secondary parts such as the spoilers, flaps, wings, engine cowls, nacelles, and ailerons [17], as presented in Figure 1.2. Recently, the automotive industry used composite panels in the floor pans and front bulkheads of the body structure [18]. Moreover, many hexagonal-shaped core structure applications are employed in sports equipment like surfboards and snowboards [4, 19]. Recent advanced lightweight composite sandwich panels are introduced for the wind turbine blades and the helicopter blades [18]. Most of these structural applications, specifically the aerospace industry, utilizes the HC core made of phenolic resin impregnated *Nomex* paper [20].

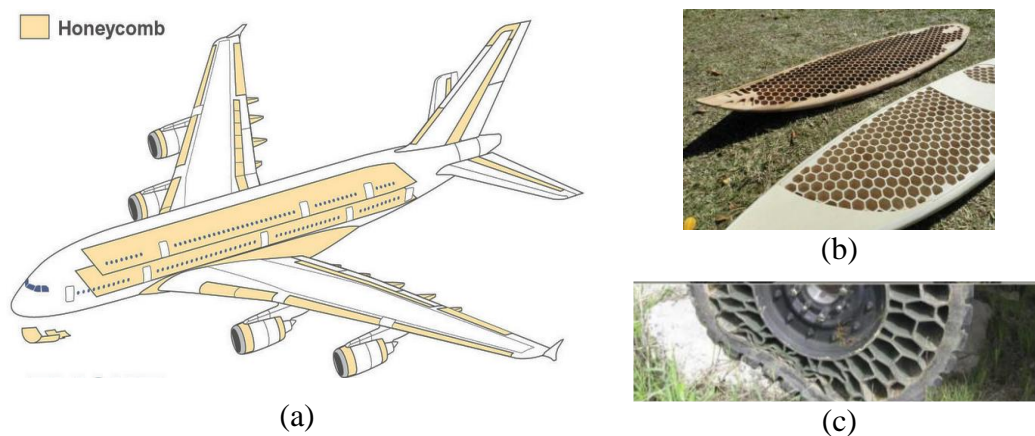


Figure 1.2 (a) HC application in airframe structure (Airbus A380), (b) wooden surfboard and (c) Non-pneumatic tire with HC spokes [21]

1.2 Research Background

The design of HC sandwich panels could be optimized with respect to the strength, stiffness, and stability requirements. The challenge is to consider the design trade-offs in the combination of lightweight materials that meet the product's strength requirements while maintaining cost-effectiveness. Thus, the industries need to evaluate the structure resistance under different loading conditions like quasi-static, fatigue and impact loading, and the failure propagation during service life. The mechanical behavior of the HC core under various loading conditions such as compression, tension, shear, and flexural loading is beneficial to measure the intrinsic properties of the core [22]. Depending on the geometric specifications, the HC core exhibits an anisotropic response under the quasi-static and low impact loading conditions [23]. Under the lateral forces, the compressive failure mode of the HC structure in the through-thickness direction and the associated localized buckling of the HC core are of primary concern. [24, 25]. In addition, the HC sandwich panel's reliability should also be considered in the presence of the fatigue loading. However, the weakest point of the core is the small adhesive area of HC cells with face sheets such that a manufacturing defect or in-service load-induced damage could easily cause debonding, leading to catastrophic failure of the HC sandwich structure [26-28]. Also, the structural properties of the HC core are relatively weaker than the high-strength face sheets in the majority of cases [11, 29]. Core deformation and failure are, therefore, decisive factors for the energy absorption capability of sandwich panels. A thorough understanding of the mechanical responses of the HC core is thus inevitable in quantifying the performance and reliability of these HC structures.

In this respect, finite element (FE) analysis is commonly employed to establish the internal states of strains and stresses during the deformation and failure process of the structure [30-33]. With the available FE tools, the need to find efficient analysis methods relies mainly on the level of understanding of the core behavior and the impact of core design on the overall behavior of the sandwich panel. The numerical modeling of the HC core structural behavior under general loading conditions has been performed at both macro-and meso/micro-length scales. The macro-mechanical approach employs an equivalent homogeneous solid. This approach does not account

for the localized buckling of the core [34-36]. The meso/micro-mechanical model utilizes the representative unit cell of the HC core [32, 37]. The models account for the details of the geometric features of the cellular structure and the cell wall material. The model takes the cell wall material properties and predicts the structural properties and behavior of the HC core panel with multiple cells. The success of the abovementioned models relies, to a great extent, on the availability of the experimentally-determined structural and material properties of the HC cores. Owing to that, the accuracy of the FE-calculated results depends, among others, on the accuracy of the geometrical model of the HC cells, prescribed boundary conditions and loading, the precision of the measured material properties, suitable constitutive laws for the face sheet and cell wall materials.

While the mechanics of the CFRP laminates for the face sheet have rigorously been studied [38-42], limited research work is available on the deformation and failure of the HC core, particularly those fabricated from the resin-impregnated papers [10, 43]. The observed localized failure leading to the final fracture of the sandwich structure necessitates the simulation of the complete deformation process to capture the observed failure mechanisms. This calls for the constitutive model of the cell wall materials with appropriate failure criteria. In this respect, several failure criteria, including Hashin [44], Tsai-Wu [45], and Tsai-Hill [46] are of particular interest for HC core made of unidirectional fiber-reinforced polymer papers. Many researchers analyzed the out-of-plane compression response of the HC core using meso-scale multi-cell representative models [47, 48], but the mechanics of deformation through damage mechanics are yet to be elaborated. The implementation of the damage mechanics approach covers the strength characteristics and the complete failure response through localized damage initiation and propagation, as already done in CFRP laminates [40, 42]. Surprisingly, this approach is not being utilized till now for the polymeric composite HC core structures. Therefore, an efficient and validated FE model of the HC core behavior is invaluable in view of the ever-increasing computational power available for design and simulation. A validated representative cell model could then be effectively used to generate the response of the HC core structure under the general loading scenarios. This limits the costly testing on the HC core samples for identifying the primary structural properties.

The numerical analysis capability of the structural products employing the HC sandwich panels requires the proper design verification prior to experimental tests and certification for deployment. Even with the revolutionary computation power, the structural analysis of the products made of tens or thousands of sandwich panels (like fairings, flappers, and spoilers in the wing of aircraft) can become very complicated. In addition, the cost and time constraints necessitate efficient virtual methods to confirm that the structural product is capable of handling the different loading conditions during its service life. Thus, the macro-mechanical modeling approach comes into consideration, termed as the homogenization of the cellular core [17, 36, 37, 49]. Instead of the detailed cellular core model, an equivalent homogenous material replaces the cellular core having the same mechanical behavior as that of the actual HC core. This approach simplifies the numerical modeling of the complex structural parts and results in reducing computational cost and time. Developing an equivalent HC core is difficult due to the complexity of the cellular core and its mechanical characteristics based on the core geometry variation. The issue becomes more complex as new composite materials are made to be used as cell wall material for the cellular HC core. Currently, some research works are conducted to establish the equivalent HC core model, and computational tools are devised to calculate the structural properties to be used for the homogenous material in the complex sandwich panel products [50]. But this field is still open for research as the challenge is concerned with the accuracy of the assumptions being used for creating the homogenous material equivalent to the actual HC core.

The present research work establishes the damage mechanics-based meso-scale representative cell model to predict structural properties and failure processes in the HC core structure under quasi-static loading conditions. Contrary to the previously developed multi-cell models consisting of a large number of cells, the smallest possible representative cell models are created with periodic boundary conditions that drastically reduce the computational time. The predicted mechanical responses and damage behavior provide the internal states of displacement, strain, and stress, referring to the explicit material phases. The in-plane and out-of-plane mechanical properties are quantified for general loading conditions like tension, compression, and shear using experimental tests and numerical analysis. Furthermore, the FE validated out-of-plane and the in-plane mechanical properties from the experimental tests are

implemented to develop a damage-based equivalent homogenous HC core model. The validation of the equivalent model is claimed by comparing measured data and FE-predicted flexure load-displacement plots of the sandwich HC panel under three-point bend load. The FE-calculated behavior acknowledges the damage initiation event and the subsequent evolution of damage to fracture of the core structure in the representative cell model and equivalent homogenous HC core (EHC) model.

1.3 Statement of Research Problem

Multiple Representative volume element (RVE) models are used in the analytical formulations by the researchers individually for the derivation of orthotropic elastic constants to generate the equivalent model for HC core [51-54]. These theoretical equations result in different calculated values for the elastic constants for the equivalent model. Also, various finite element models are created using the meso/micro-scale representative structure of the HC core [55, 56]. FE tools are devised to replace the real HC core with the equivalent material model using the single-cell representative structure of hexagonal HC core, but that provides the initial approximation of the elastic constants for stiffness matrix [50]. Most of the open literature focused on characterizing the mechanical behavior under static or impact loading using different geometric parameters of the hexagonal honeycomb core [57-60]. But the combined effects of certain geometric parameters like cell size and cell height are yet to be quantified. To the author's knowledge, far too little attention has been given to the damage-based mechanics of deformation in paper-made honeycomb cores. These attributes can be very interesting in analyzing the failure of the honeycomb core under different loading conditions. In addition to these primary data, systematic studies are still needed for the mechanical behavior of a single honeycomb core geometry under all in-plane and out-of-plane quasi-static loading conditions. This could provide a complete set of effective elastic properties to develop an equivalent HC core model. This research aims to provide a methodology to develop a predictive model for the failure in *Nomex* HC core using a damage mechanics-based representative cell model. The structural properties from this damage mechanics-based predictive model are used as input to create an equivalent model for replacing the

cellular HC core in the sandwich panel that duplicates the real HC core behavior under any loading condition. Therefore, the research gap could be summarized to answer the following research problem. “*How effectively the HC core in the sandwich panel could be replaced with a homogenous material using a damage mechanics approach resulting in the same mechanical behavior of the real composite sandwich panel?*”

1.4 Research Objectives

The research aims to develop a verified damage mechanics-based model for deformation and failure prediction of honeycomb structures. The specific objectives of the research are :

- i. To establish relevant material properties and behavior of Honeycomb (HC) core used in the sandwich panels.
- ii. To determine the effects of geometric parameters for the structural characterization of hexagonal *Nomex* HC core under the out-of-plane compression loading.
- iii. To develop the damage mechanics-based model using meso-scale Representative Cell (RC) structure for the HC core.
- iv. To verify the damage mechanics-based FE model for the equivalent homogenized honeycomb (EHC) core structure.

1.5 Scope of the study

The present study focuses on developing a damage mechanics-based representative cell model of *Nomex* HC core that could efficiently predict the

mechanical response of the real structure under different loading conditions. The research is limited to the following scope of work:

- i. Conduct the mechanical testing for material and structural characterization of the hexagonal HC core.
 - a. Phenolic resin impregnated *Nomex* paper (type 410) specimens are used for the tension test to obtain the material properties. The overall dimension of the specimen was 350 mm (length) x 50 mm (width) with a paper thickness of 0.05 mm. The tension load was applied in the paper roll (0°) and transverse (90°) direction.
 - b. Bare *Nomex* HC core (HRH-10) specimen (cell size = 3.2 mm, height = 12.7 mm and density 64 kg/m^3) with square (30 mm x 30 mm to 70 mm x 70 mm) and rectangular (150 mm x 50 mm) cross-section are cut from the HC core panels of real aerospace structural parts. The square specimen is used for quasi-static out-of-plane compression, while the rectangular specimen is employed in the in-plane tension, shear, and out-of-plane shear loading.
 - c. Sandwich HC panel specimen comprised of CFRP 2-ply $[0]_2$ and 8-ply $[0]_8$ face sheets and *Nomex* HC core with same cell size and height as above. These sandwich panels were cut into a square (50 mm x 50 mm) and rectangular (200 mm x 75 mm) cross-section. The square sandwich specimen (with 8-ply CFRP face sheets) is used for quasi-static out-of-plane tension, while the rectangular sandwich panel (with 2-ply CFRP face sheets) for the quasi-static three-point bend experiment.
- ii. Parametric analysis of bare HC core structures is conducted using different cellular configurations for out-of-plane compression. Specimen with cell size (3.2 mm, 4.8 mm), core height (8 mm, 12.7 mm, 18 mm) and density (32 kg/m^3 , 64 kg/m^3 , 128 kg/m^3) are used for the compression testing.
- iii. Damage-based finite element representative cell models are developed by using ABAQUS 6.14. Hashin damage criteria with energy-based damage

evolution is implemented to simulate the following quasi-static out-of-plane loading cases:

- a. Tension and compression load cases are simulated using hexagonal cell configurations of single-cell, 4-cell, and 24-cell models.
 - b. A shear load case model was created using a 6-cell configuration of hexagonal HC core. The shear load case is comprised of the ribbon and transverse direction.
- iv. A Hybrid experimental-computational approach is adapted to obtain the effective structural properties of hexagonal *Nomex* HC core. The in-plane structural properties are taken directly from mechanical testing, while the out-of-plane structural responses are validated through representative cell models. These both are used as input to create the following damage mechanics-based equivalent homogenized HC core models.
- a. Multi-cell equivalent model with geometric dimensions of 50 mm x 50 mm x 12.7 mm is simulated using the said structural properties for quasi-static compression load.
 - b. Single-cell equivalent model with a geometric configuration of 5.54 mm x 3.36 mm x 12.7 mm is created, and numerical analysis is performed to assess the deformation and failure process, respectively.
 - c. Verification of the newly developed damage-based equivalent HC core model is done by simulating the quasi-static three-point bend loading of sandwich HC panel. The localized structural deformation and damage evolution to fracture of the HC core is analyzed in detail for the respective loading condition.

1.6 Significance of the Study

This research work presents a methodology for replacing the cellular HC with the equivalent homogenous structure that effectively predicts the mechanical behavior of the real HC core. The developed equivalent homogenized honeycomb core (EHC) model significantly reduced the model size, which lowers the computational time and cost for the whole composite sandwich panel. The validated model acknowledges the gradual accumulation of material damage leading to crack initiation of material points in the equivalent model. In addition, the methodology can be adapted for other polymer-based materials with available experimental data. Moreover, the research also provides an in-depth understanding of failure mechanics by using damage-based representative cell models. The representative cell models are formed using the smallest possible unit-cell structure that efficiently predicted the material point damage under different loading conditions. The verified methodology for the representative cell and the EHC models will be significant for all the industries associated with lightweight structures, specifically the aerospace companies such as Composite Technology Research Malaysia (CTRM) and transport industries as well. The representative cell model methodology could be useful for these companies in conducting the computational analysis instead of experimental testing that could save high product development cost and time for different aircraft parts. The damage mechanics-based approach implemented in these models helps in quantifying the real HC core mechanical response. This is of immense significance in the computational analysis of large complex structures where the computational time and cost are of utmost importance.

1.7 Thesis Layout

This thesis consists of eight chapters. All the chapters are arranged to establish an equivalent homogenized HC core model for predicting the deformation response under different loading conditions. The validated damage mechanics-based finite element methodology is described for representing actual HC core behavior through a

homogenous model using structural properties. Each chapter's content is specified here to link them with the specific objectives and scope of the research.

In Chapter 1, the research background and challenges in numerical analysis relate to the complexity of the anisotropic *Nomex* honeycomb core structures used in sandwich panels for automotive and aerospace industries. The problem statement, specific objectives, and significance are clarified. The limits of this research are defined in the scope of the study.

Chapter 2 summarizes the literature on honeycomb core structures, mechanical properties, and behavior under quasi-static loading. Existing numerical tools and FE procedures to predict the failure response are covered. Various representative cell models are identified from literature used in previous studies to predict the deformation and failure. Different homogenization models are discussed that were created to replace cellular honeycomb core structure as an equivalent material. Previous research based on theoretical models to find elastic constants for stiffness matrix are described. All this literature review is given in detail to have an insight on the current topic and provide the basis for further research needed in this specific area.

Chapter 3 provides the detailed research methodology of the current study. A hybrid experimental-computational approach is established to find the structural properties of hexagonal *Nomex* HC core. Firstly, validated damage mechanics-based representative cell model formation is elaborated for the out-of-plane loading conditions. The representative cell model consists of the real hexagonal HC core geometry. Then, the creation of damage mechanics-based equivalent homogenized HC core model methodology is explained in which the HC core is replaced by equivalent homogenous material that will duplicate the real HC structure behavior. The detailed information of validating the equivalent model through three-point bend loading on the sandwich HC panels is described.

Chapter 4 consists of all the experimental test results that relate to HC core structures. First, the phenolic resin-based *Nomex* paper tensile properties are described. The orthotropic elastic constants along-with the damage parameters are extracted that

are to be used as input for the damage mechanics-based representative cell model of the HC core. Secondly, the out-of-plane tension, compression, and shear deformation are presented for the respective HC core, while the global load-displacement responses are plotted to quantify the mechanical properties. Then, the in-plane tension and shear deformation results are described for the same geometry of HC core structure. The catastrophic damage to different loading conditions is explained through the mechanics of deformation and failure for each loading case. In the last section, the three-point bend experimental test results of sandwich HC panel are given that will be used for validation of equivalent homogenized HC core model.

In Chapter 5, the parametric analysis of the HC core structure is provided for the out-of-plane compression behavior. The influence of HC geometry, particularly the cell size, the height of core, and relative density, are analyzed and discussed individually. Then, the effects of cell aspect ratio (height/cell size) and relative density on the compression modulus, strength, and dissipation energy are established. A phenomenological model is presented that could effectively predict the compressive strength of the *Nomex* HC core using the combined effects of relative density and cell aspect ratio.

Chapter 6 describes the developed representative cell model numerical results for the HC core out-of-plane loading conditions. The mechanical responses of the damage mechanics-based models consisting of single-cell and multiple hexagonal cells of the HC core are presented in detail. The FE-calculated behavior acknowledges the damage initiation followed by the damage evolution to fracture of the HC core. The representative cell models are validated experimentally for each respective load case and cover both mechanics of materials and the deformation mechanism. It is clarified that the mechanical deformation responses could be efficiently predicted by the smallest possible representative cell model of hexagonal HC core using the damage mechanics approach.

Chapter 7 elaborates the numerical analysis of damage-based homogenous equivalent homogenized honeycomb core (EHC) models. The computational results of equivalent multi-cell and single-cell models are assessed to examine the developed

homogenization technique through structural properties. The load-displacement plots and the progressive damage in the EHC models are described for each case. A numerical model of the three-point bend loading condition for sandwich HC panel is done in the last section. The sandwich panel is modeled to have stiff CFRP face sheets bonded to equivalent HC core surfaces, and a three-point load is applied. The EHC model results are compared with the measured response. The computational results are shown to be in accordance with the measured data, and the EHC model replicated the exact mechanical behavior of the real HC core.

Chapter 8 summarizes the main conclusion related to the methodology adopted for the representative cell model. Furthermore, the verified EHC model responses are concluded. The main contributions that are addressed in the form of research objectives are concluded in this chapter. Further research recommendations are listed to increase the knowledge base in the field of HC structures.

REFERENCES

1. Bitzer T. Honeycomb technology: materials, design, manufacturing, applications and testing: Springer Science & Business Media; 2012.
2. Grediac M. A finite element study of the transverse shear in honeycomb cores. *International journal of solids and structures*. 1993;30(13):1777-88.
3. Menta V, Vuppalapati R, Chandrashekhara K, Pfitzinger D, Phan N. Manufacturing and mechanical performance evaluation of resin-infused honeycomb composites. *Journal of Reinforced Plastics and Composites*. 2012;31(6):415-23.
4. Zhang Q, Yang X, Li P, Huang G, Feng S, Shen C, et al. Bioinspired engineering of honeycomb structure—Using nature to inspire human innovation. *Progress in Materials Science*. 2015;74:332-400.
5. Cote F, Deshpande V, Fleck N, Evans A. The out-of-plane compressive behavior of metallic honeycombs. *Materials Science and Engineering: A*. 2004;380(1-2):272-80.
6. Crupi V, Epasto G, Guglielmino E. Comparison of aluminium sandwiches for lightweight ship structures: Honeycomb vs. foam. *Marine structures*. 2013;30:74-96.
7. Wang Z, Tian H, Lu Z, Zhou W. High-speed axial impact of aluminum honeycomb—Experiments and simulations. *Composites Part B: Engineering*. 2014;56:1-8.
8. Nomoto K. Aramid honeycombs and a method for producing the same. European patent specification (EP 1 152 084 B1). 2001.
9. Zhou Z, Wang Z, Zhao L, Shu X. Experimental investigation on the yield behavior of Nomex honeycombs under combined shear-compression. *Latin American Journal of Solids and Structures*. 2012;9(4):515-30.
10. Liu L, Meng P, Wang H, Guan Z. The flatwise compressive properties of Nomex honeycomb core with debonding imperfections in the double cell wall. *Composites Part B: Engineering*. 2015;76:122-32.
11. Rodríguez-Ramírez JdD, Castanié B, Bouvet C. Damage Mechanics Modelling of the shear nonlinear behavior of Nomex honeycomb core. Application to sandwich beams. *Mechanics of Advanced Materials and Structures*. 2020;27(1):80-9.

12. Paik JK, Thayamballi AK, Kim GS. The strength characteristics of aluminum honeycomb sandwich panels. *Thin-walled structures*. 1999;35(3):205-31.
13. Belouettar S, Abbadi A, Azari Z, Belouettar R, Freres P. Experimental investigation of static and fatigue behaviour of composites honeycomb materials using four point bending tests. *Composite Structures*. 2009;87(3):265-73.
14. Yang Y, Fallah A, Saunders M, Louca L. On the dynamic response of sandwich panels with different core set-ups subject to global and local blast loads. *Engineering Structures*. 2011;33(10):2781-93.
15. Katunin A, John M, Jozsko K, Kajzer A. Characterization of quasi-static behavior of honeycomb core sandwich structures.“. *Modelowanie Inżynierskie*. 2014;22:78-84.
16. Farooq U, Khurram A, Ahmad M, Rakha S, Ali N, Munir A, et al., editors. Optimization of the manufacturing parameters of honeycomb composite sandwich structures for aerospace application. 2013 International Conference on Aerospace Science & Engineering (ICASE); 2013: IEEE.
17. Middleton D. *Composite Materials in Aircraft Structures*, 1990. Longman Scientific and Technical, London.
18. Nast E, Nast E, editors. On honeycomb-type core moduli. 38th Structures, Structural Dynamics, and Materials Conference; 1997.
19. Warren AT, Kosasih B, Gibson CR, Beirne ST, Steele JR. Surfing the 3D printing wave: the changing face of surfboard fin production. 2017.
20. Kindinger J. Lightweight structural cores. *ASM Handbook*. 2001;21(180-183):237.
21. Jin X, Hou C, Fan X, Sun Y, Lv J, Lu C. Investigation on the static and dynamic behaviors of non-pneumatic tires with honeycomb spokes. *Composite Structures*. 2018;187:27-35.
22. Gibson LJ, Ashby MF. *Cellular solids: structure and properties*: Cambridge university press; 1999.
23. Herrmann C, Dewulf W, Hauschild M, Kaluza A, Kara S, Skerlos S. Life cycle engineering of lightweight structures. *CIRP Annals*. 2018;67(2):651-72.
24. Foo CC, Chai GB, Seah LK. Mechanical properties of Nomex material and Nomex honeycomb structure. *Composite structures*. 2007;80(4):588-94.

25. Roy R, Park S-J, Kweon J-H, Choi J-H. Characterization of Nomex honeycomb core constituent material mechanical properties. *Composite Structures*. 2014;117:255-66.
26. Khan S, Loken H. Bonding of sandwich structures—the facesheet/honeycomb interface—a phenomenological study. *Proceedings of SAMPE*. 2007:1-9.
27. Kaman MO, Solmaz MY, Turan K. Experimental and numerical analysis of critical buckling load of honeycomb sandwich panels. *Journal of composite materials*. 2010;44(24):2819-31.
28. Akour S, Maaitah H. Finite element analysis of loading area effect on sandwich panel behaviour beyond the yield limit. *Finite Element Analysis—New Trends and Developments*, F Ebrahimi (Ed), InTech, Rijeka, Croatia. 2012.
29. Seemann R, Krause D, editors. Numerical modelling of nomex honeycomb cores for detailed analyses of sandwich panel joints. *11th World Congress on Computational Mechanics (WCCM XI)*; 2014.
30. Lee HS, Hong SH, Lee JR, Kim YK. Mechanical behavior and failure process during compressive and shear deformation of honeycomb composite at elevated temperatures. *Journal of Materials Science*. 2002;37(6):1265-72.
31. Aminanda Y, Castanié B, Barrau J-J, Thevenet P. Experimental analysis and modeling of the crushing of honeycomb cores. *Applied Composite Materials*. 2005;12(3-4):213-27.
32. Heimbs S. Virtual testing of sandwich core structures using dynamic finite element simulations. *Computational Materials Science*. 2009;45(2):205-16.
33. Castanié B, Aminanda Y, Barrau J-J, Thevenet P. Discrete Modeling of the Crushing of Nomex Honeycomb Core and Application to Impact and Post-impact Behavior of Sandwich Structures. *Dynamic Failure of Composite and Sandwich Structures*: Springer; 2013. p. 427-89.
34. Foo C, Chai G, Seah L. A model to predict low-velocity impact response and damage in sandwich composites. *Composites Science and Technology*. 2008;68(6):1348-56.
35. Asprone D, Auricchio F, Menna C, Morganti S, Prota A, Reali A. Statistical finite element analysis of the buckling behavior of honeycomb structures. *Composite Structures*. 2013;105:240-55.
36. Malek S, Gibson L. Effective elastic properties of periodic hexagonal honeycombs. *Mechanics of Materials*. 2015;91:226-40.

37. Sorohan Ş, Sandu M, Sandu A, Constantinescu DM. Finite Element Models Used to Determine the Equivalent In-plane Properties of Honeycombs. *Materials Today: Proceedings*. 2016;3(4):1161-6.
38. Sun C, Tao J. Prediction of failure envelopes and stress/strain behaviour of composite laminates. *Composites Science and technology*. 1998;58(7):1125-36.
39. Sun C. Strength analysis of unidirectional composites and laminates. 2000.
40. Kolor S, Khosravani MR, Hamzah R, Tamin M. FE model-based construction and progressive damage processes of FRP composite laminates with different manufacturing processes. *International Journal of Mechanical Sciences*. 2018;141:223-35.
41. Kolor S, Tamin M. Mode-II interlaminar fracture and crack-jump phenomenon in CFRP composite laminate materials. *Composite Structures*. 2018;204:594-606.
42. Rahimian Kolor SS, Karimzadeh A, Yidris N, Petru M, Ayatollahi MR, Tamin MN. An energy-based concept for yielding of multidirectional FRP composite structures using a mesoscale lamina damage model. *Polymers*. 2020;12(1):157.
43. Fischer S, Drechsler K, Kilchert S, Johnson A. Mechanical tests for foldcore base material properties. *Composites Part A: Applied Science and Manufacturing*. 2009;40(12):1941-52.
44. Hashin Z. Failure criteria for unidirectional fiber composites. *Journal of Applied Mechanics*. 1980;47:329-34.
45. Li S, Sitnikova E, Liang Y, Kaddour A-S. The Tsai-Wu failure criterion rationalised in the context of UD composites. *Composites Part A: Applied Science and Manufacturing*. 2017;102:207-17.
46. Fuchs C, Bhattacharyya D, Fakirov S. Microfibril reinforced polymer–polymer composites: Application of Tsai-Hill equation to PP/PET composites. *Composites science and technology*. 2006;66(16):3161-71.
47. Roy R, Kweon J, Choi J. Meso-scale finite element modeling of Nomex™ honeycomb cores. *Advanced Composite Materials*. 2014;23(1):17-29.
48. Sun G, Huo X, Chen D, Li Q. Experimental and numerical study on honeycomb sandwich panels under bending and in-panel compression. *Materials & Design*. 2017;133:154-68.

49. Li Y, Abbès F, Hoang M, Abbès B, Guo Y. Analytical homogenization for in-plane shear, torsion and transverse shear of honeycomb core with skin and thickness effects. *Composite Structures*. 2016;140:453-62.
50. Gornet L, Marguet S, Marckmann G. Finite Element modeling of Nomex® honeycomb cores: Failure and effective elastic properties. *International Journal Computer Material & Continua Tech Science*. 2006;1:11-22.
51. Gibson LJ, Ashby MF, Schajer G, Robertson C. The mechanics of two-dimensional cellular materials. *Proceedings of the Royal Society of London A Mathematical and Physical Sciences*. 1982;382(1782):25-42.
52. Zhang J, Ashby M. The out-of-plane properties of honeycombs. *International Journal of Mechanical Sciences*. 1992;34(6):475-89.
53. Shi G, Tong P. The derivation of equivalent constitutive equations of honeycomb structures by a two scale method. *Computational mechanics*. 1995;15(5):395-407.
54. Masters I, Evans K. Models for the elastic deformation of honeycombs. *Composite structures*. 1996;35(4):403-22.
55. Mukherjee G, Saraf M. Studies on a fiber reinforced plastics honeycomb structure. *Polymer composites*. 1994;15(3):217-22.
56. Słonina M, Dziurka D, Smardzewski J. Experimental Research and Numerical Analysis of the Elastic Properties of Paper Cell Cores before and after Impregnation. *Materials*. 2020;13(9):2058.
57. Lee SM, Tsotsis TK. Indentation failure behavior of honeycomb sandwich panels. *Composites science and technology*. 2000;60(8):1147-59.
58. Zhou Q, Mayer RR. Characterization of aluminum honeycomb material failure in large deformation compression, shear, and tearing. *Journal of Engineering Materials and Technology*. 2002;124(4):412-20.
59. Mahmoudabadi MZ, Sadighi M. A theoretical and experimental study on metal hexagonal honeycomb crushing under quasi-static and low velocity impact loading. *Materials Science and Engineering: A*. 2011;528(15):4958-66.
60. Giunta G, Catapano A, Belouettar S. Failure indentation analysis of composite sandwich plates via hierarchical models. *Journal of Sandwich Structures & Materials*. 2013;15(1):45-70.
61. Aktay L, Johnson AF, Kröplin B-H. Numerical modelling of honeycomb core crush behaviour. *Engineering Fracture Mechanics*. 2008;75(9):2616-30.

62. Lamb A. Experimental investigation and numerical modelling of composite-honeycomb materials used in formula 1 crash structures. 2007.
63. Meraghni F, Desrumaux F, Benzeggagh M. Mechanical behaviour of cellular core for structural sandwich panels. *Composites Part A: Applied Science and Manufacturing*. 1999;30(6):767-79.
64. Giglio M, Manes A, Gilioli A. Investigations on sandwich core properties through an experimental–numerical approach. *Composites Part B: Engineering*. 2012;43(2):361-74.
65. Goswami S, Becker W. Analysis of debonding fracture in a sandwich plate with hexagonal core. *Composite structures*. 2000;49(4):385-92.
66. Akay M, Hanna R. A comparison of honeycomb-core and foam-core carbon-fibre/epoxy sandwich panels. *Composites*. 1990;21(4):325-31.
67. Minguet P, Dugundji J, Lagace PA. Buckling and failure of sandwich plates with graphite-epoxy faces and various cores. *Journal of Aircraft*. 1988;25(4):372-9.
68. Soliman H. Mechanical properties of cellular core structures: Virginia Tech; 2016.
69. Composites H. HexWeb™ Honeycomb Attributes and Properties, A comprehensive guide to standard Hexcel honeycomb materials, configurations, and mechanical properties. *Honeycomb Data Sheets*. 1999.
70. Gibson L. Ashby, MF: *Cellular Solids. Structure and Properties* Oxford: Pergamon Press. 1988.
71. Velea MN, Lache S. Numerical simulations of the mechanical behavior of various periodic cellular cores for sandwich panels. *Procedia Engineering*. 2011;10:287-92.
72. Velea MN, Lache S. In-plane effective elastic properties of a novel cellular core for sandwich structures. *Mechanics of Materials*. 2011;43(7):377-88.
73. Velea MN, Wennhage P, Lache S. Out-of-plane effective shear elastic properties of a novel cellular core for sandwich structures. *Materials & Design (1980-2015)*. 2012;36:679-86.
74. Lee B-C, Lee K-W, Byun J-H, Kang K-J. The compressive response of new composite truss cores. *Composites Part B: Engineering*. 2012;43(2):317-24.
75. Ueng C, Underwood E, Liu T. Shear Modulus of New Sandwich Cores. *AIAA Journal*. 1980;18(6):721-3.

76. Grenestedt JL. Effective elastic behavior of some models for perfect cellular solids. *International Journal of Solids and Structures*. 1999;36(10):1471-501.
77. He L, Cheng Y-S, Liu J. Precise bending stress analysis of corrugated-core, honeycomb-core and X-core sandwich panels. *Composite Structures*. 2012;94(5):1656-68.
78. Pan S-D, Wu L-Z, Sun Y-G, Zhou Z-G, Qu J-L. Longitudinal shear strength and failure process of honeycomb cores. *Composite Structures*. 2006;72(1):42-6.
79. Pan S-D, Wu L-Z, Sun Y-G. Transverse shear modulus and strength of honeycomb cores. *Composite Structures*. 2008;84(4):369-74.
80. Soltani A, Noroozi R, Bodaghi M, Zolfagharian A, Hedayati R. 3D printing on-water sports boards with bio-inspired core designs. *Polymers*. 2020;12(1):250.
81. Zaharia SM, Enescu LA, Pop MA. Mechanical Performances of lightweight sandwich structures produced by material extrusion-based additive manufacturing. *Polymers*. 2020;12(8):1740.
82. Saad NA, Sabah A, editors. An investigation of new design of light weight structure of (ABS/PLA) by using of three dimensions printing. *Proceedings of the 13th International Conference "Standardization, Prototypes and Quality: A Means of Balkan Countries' Collaboration"*, Brasov, Romania; 2016.
83. Ashab A, Ruan D, Lu G, Xu S, Wen C. Experimental investigation of the mechanical behavior of aluminum honeycombs under quasi-static and dynamic indentation. *Materials & Design*. 2015;74:138-49.
84. Ivañez I, Fernandez-Cañadas LM, Sanchez-Saez S. Compressive deformation and energy-absorption capability of aluminium honeycomb core. *Composite Structures*. 2017;174:123-33.
85. Andrews M, Lu D, Young R. Compressive properties of aramid fibres. *Polymer*. 1997;38(10):2379-88.
86. Giglio M, Gilioli A, Manes A. Numerical investigation of a three point bending test on sandwich panels with aluminum skins and Nomex™ honeycomb core. *Computational Materials Science*. 2012;56:69-78.
87. Manes A, Gilioli A, Sbarufatti C, Giglio M. Experimental and numerical investigations of low velocity impact on sandwich panels. *Composite Structures*. 2013;99:8-18.

88. Castanié B, Bouvet C, Aminanda Y, Barrau J-J, Thévenet P. Modelling of low-energy/low-velocity impact on Nomex honeycomb sandwich structures with metallic skins. *International Journal of Impact Engineering*. 2008;35(7):620-34.
89. Liu L, Wang H, Guan Z. Experimental and numerical study on the mechanical response of Nomex honeycomb core under transverse loading. *Composite Structures*. 2015;121:304-14.
90. Standard A. D638–03. 'Standard Test Method for Tensile Properties of Plastics', West Conshohocken, PA: ASTM International. DOI 10.1520/D0638-03, www.astm.org (2003, accessed July 2011).
91. Kim KS, Chin I-J, Sung IK, Min KS. Curing of Nomex/phenolic and Kraft/Phenolic honeycombs. *Korea Polymer Journal*. 1995;3(1):35-40.
92. Tsujii Y, Tanaka K, Nishida Y. Analysis of mechanical properties of aramid honeycomb core. *Trans Jpn Soc Mech Eng*. 1995;61:1608-14.
93. Hähnel F, Wolf K, editors. Evaluation of the material properties of resin-impregnated Nomex paper as basis for the simulation of the impact behaviour of honeycomb sandwich. *Proceedings of the 3rd international conference on composites testing and model identification*; 2006: Citeseer.
94. Seemann R, Krause D. Numerical modelling of Nomex honeycomb sandwich cores at meso-scale level. *Composite Structures*. 2017;159:702-18.
95. Torquato S, Gibiansky L, Silva M, Gibson L. Effective mechanical and transport properties of cellular solids. *International Journal of Mechanical Sciences*. 1998;40(1):71-82.
96. Becker W. Closed-form analysis of the thickness effect of regular honeycomb core material. *Composite structures*. 2000;48(1-3):67-70.
97. Balawi S, Abot J. The effect of honeycomb relative density on its effective in-plane elastic moduli: An experimental study. *Composite Structures*. 2008;84(4):293-9.
98. Balawi S, Abot J. A refined model for the effective in-plane elastic moduli of hexagonal honeycombs. *Composite Structures*. 2008;84(2):147-58.
99. Chen D, Ozaki S. Analysis of in-plane elastic modulus for a hexagonal honeycomb core: Effect of core height and proposed analytical method. *Composite Structures*. 2009;88(1):17-25.
100. Dai G, Zhang W. Cell size effect analysis of the effective Young's modulus of sandwich core. *Computational materials science*. 2009;46(3):744-8.

101. You J, Zhang H, Zhu H, Kennedy D. The high strain compression of micro- and nano-sized random irregular honeycombs. *Materials Research Express*. 2016;3(9):095023.
102. Penzien J, Didriksson T. Effective shear modulus of honeycomb cellular structure. *AIAA Journal*. 1964;2(3):531-5.
103. Qiao P, Fan W, Davalos JF, Zou G. Optimization of transverse shear moduli for composite honeycomb cores. *Composite structures*. 2008;85(3):265-74.
104. Xu XF, Qiao P, Davalos JF. Transverse shear stiffness of composite honeycomb core with general configuration. *Journal of engineering mechanics*. 2001;127(11):1144-51.
105. Staal RA. Failure of sandwich honeycomb panels in bending: ResearchSpace@ Auckland; 2006.
106. C297. AS. Standard test method for flatwise tensile strength of sandwich constructions. ASTM International 2004.
107. Heimbs S, Middendorf P, Maier M, editors. Honeycomb sandwich material modeling for dynamic simulations of aircraft interior components. 9th international LS-DYNA users conference; 2006.
108. Qiu K, Wang Z, Zhang W. The effective elastic properties of flexible hexagonal honeycomb cores with consideration for geometric nonlinearity. *Aerospace Science and Technology*. 2016;58:258-66.
109. Takeda N, Minakuchi S, Okabe Y. Smart composite sandwich structures for future aerospace application-Damage detection and suppression-: A review. *Journal of Solid Mechanics and Materials Engineering*. 2007;1(1):3-17.
110. Roy R, Nguyen K, Park Y, Kweon J, Choi J. Testing and modeling of Nomex™ honeycomb sandwich Panels with bolt insert. *Composites Part B: Engineering*. 2014;56:762-9.
111. Wierzbicki T. Crushing analysis of metal honeycombs. *International Journal of Impact Engineering*. 1983;1(2):157-74.
112. Kreja I. A literature review on computational models for laminated composite and sandwich panels. *Open Engineering*. 2011;1(1):59-80.
113. Hu L, You F, Yu T. Effect of cell-wall angle on the in-plane crushing behaviour of hexagonal honeycombs. *Materials & Design*. 2013;46:511-23.

114. Khan MS, Kolor SSR, Tamin MN. Effects of cell aspect ratio and relative density on deformation response and failure of honeycomb core structure. *Materials Research Express*. 2020;7(1):015332.
115. Kmita-Fudalej G, Szewczyk W, Kołakowski Z. Calculation of Honeycomb Paperboard Resistance to Edge Crush Test. *Materials*. 2020;13(7):1706.
116. Shahverdi H, Barati MR, Hakimelahi B. Post-buckling analysis of honeycomb core sandwich panels with geometrical imperfection and graphene reinforced nano-composite face sheets. *Materials Research Express*. 2019;6(9):095017.
117. Grenestedt JL, Bassinet F. Influence of cell wall thickness variations on elastic stiffness of closed-cell cellular solids. *International Journal of Mechanical Sciences*. 2000;42(7):1327-38.
118. Bunyawanichakul P, Castanié B, Barrau J-J. Experimental and numerical analysis of inserts in sandwich structures. *Applied Composite Materials*. 2005;12(3):177-91.
119. Heimbs S, Pein M. Failure behaviour of honeycomb sandwich corner joints and inserts. *Composite Structures*. 2009;89(4):575-88.
120. Kress G, Winkler M. Honeycomb sandwich residual stress deformation pattern. *Composite structures*. 2009;89(2):294-302.
121. Becker W. The in-plane stiffnesses of a honeycomb core including the thickness effect. *Archive of Applied Mechanics*. 1998;68(5):334-41.
122. Marfia S, Sacco E. Micromechanics and homogenization of SMA-wire-reinforced materials. *J Appl Mech*. 2005;72(2):259-68.
123. Charalambakis N. Homogenization techniques and micromechanics. A survey and perspectives. *Applied Mechanics Reviews*. 2010;63(3).
124. Venkatesan KRR, Rai A, Stoumbos TG, Inoyama D, Chattopadhyay A, editors. Finite element based damage and failure analysis of honeycomb core sandwich composite structures for space applications. *AIAA Scitech 2020 Forum*; 2020.
125. Heimbs S. Sandwichstrukturen mit Wabenkern: Experimentelle und numerische Analyse des Schädigungsverhaltens unter statischer und kurzzeitdynamischer Belastung. 2008.
126. Bunyawanichakul P, Castanié B, Barrau J-J. Non-linear finite element analysis of inserts in composite sandwich structures. *Composites Part B: Engineering*. 2008;39(7-8):1077-92.

127. Allegri G, Lecci U, Marchetti M, Poscente F, editors. FEM simulation of the mechanical behaviour of sandwich materials for aerospace structures. Key Engineering Materials; 2002: Trans Tech Publ.
128. Ivañez I, Moure M, Garcia-Castillo SK, Sanchez-Saez S. The oblique impact response of composite sandwich plates. Composite structures. 2015;133:1127-36.
129. Jaafar M, Atlati S, Makich H, Nouari M, Moufki A, Julliere B. A 3D FE modeling of machining process of Nomex® honeycomb core: influence of the cell structure behaviour and specific tool geometry. Procedia Cirp. 2017;58:505-10.
130. Gornet L, Marckmann G, Ollier G. Interactions modèles expériences sur des âmes nids d'abeilles Nomex (R): application au design d'un voilier multicoque de course océanique. Revue des composites et des matériaux avancés. 2006;16(2):167-90.
131. Płatek P, Rajkowski K, Cieplak K, Sarzyński M, Małachowski J, Woźniak R, et al. Deformation Process of 3D Printed Structures Made from Flexible Material with Different Values of Relative Density. Polymers. 2020;12(9):2120.
132. Mazhar F, Khan A, editors. Structural design of a uav wing using finite element method. 51st AIAA/ASME/ASCE/AHS/ASC Structures, Structural Dynamics, and Materials Conference 18th AIAA/ASME/AHS Adaptive Structures Conference 12th; 2010.
133. Zhu J-H, Zhang W-H, Xia L. Topology optimization in aircraft and aerospace structures design. Archives of Computational Methods in Engineering. 2016;23(4):595-622.
134. Murakami S. Continuum damage mechanics: a continuum mechanics approach to the analysis of damage and fracture: Springer Science & Business Media; 2012.
135. Kolor R. SS Simulation Methodology for Fracture Processes of Composite Laminates Using Damage-Based Models. Department of design and applied mechanics, faculty of mechanical engineering: Universiti Teknologi Malaysia, Johor; 2016.
136. Cowin SC. Continuum mechanics of anisotropic materials: Springer Science & Business Media; 2013.
137. Dharan C. Fracture mechanics of composite materials. 1978.
138. Sadowski T. Modelling of damage and fracture processes of ceramic matrix composites under mechanical loading. Multiscale Modeling of Complex Materials: Springer; 2014. p. 151-78.

139. Zhang Y, Yang C. Recent developments in finite element analysis for laminated composite plates. *Composite structures*. 2009;88(1):147-57.
140. Orifici AC, Herszberg I, Thomson RS. Review of methodologies for composite material modelling incorporating failure. *Composite structures*. 2008;86(1-3):194-210.
141. Hinton M, Soden P. Predicting failure in composite laminates: the background to the exercise. *Composites Science and Technology*. 1998;58(7):1001-10.
142. Tsai SW, Wu EM. A general theory of strength for anisotropic materials. *Journal of composite materials*. 1971;5(1):58-80.
143. Camanho PP, Dávila CG. Mixed-mode decohesion finite elements for the simulation of delamination in composite materials. 2002.
144. Sun C-T. COMPARATIVE EVALUATION OF FAILURE ANALYSIS METHODS FOR COMPOSITE LAMINATES. 1996.
145. Hashin Z, Rotem A. A fatigue failure criterion for fiber reinforced materials. *Journal of composite materials*. 1973;7(4):448-64.
146. Abdullah M. Delamination damage of carbon fiber-reinforced polymer composite laminates under cyclic shear-induced loading conditions: *Universiti Teknologi Malaysia*; 2018.
147. Gornet L, Marguet S, Marckmann G. Modeling of Nomex® honeycomb cores, linear and nonlinear behaviors. *Mechanics of advanced Materials and structures*. 2007;14(8):589-601.
148. Yang G. Experimental investigation of strength criteria for S-glass, E-glass and graphite fiber composite plate. *Theoretical and applied fracture mechanics*. 1994;20(1):59-66.
149. Ijaz H, Saleem W, Zain-ul-Abdein M, Mabrouki T, Rubaiee S, Salmeen Bin Mahfouz A. Finite element analysis of bend test of sandwich structures using strain energy based homogenization method. *Advances in Materials Science and Engineering*. 2017;2017.
150. Aborehab A, Kassem M, Nemnem A, Kamel M. Miscellaneous Modeling Approaches and Testing of a Satellite Honeycomb Sandwich Plate. *Journal of Applied and Computational Mechanics*. 2019.
151. Karlsson U. Ekvivalenta styvhetsparametrar för honeycomb 1987.
152. Martinez RM. Apparent properties of a honeycomb core sandwich panel by numerical experiment. 2001.

153. Liu Q, Zhao Y. Effect of soft honeycomb core on flexural vibration of sandwich panel using low order and high order shear deformation models. *Journal of Sandwich Structures & Materials*. 2007;9(1):95-108.
154. Steenackers G, Peeters J, Ribbens B, Vuye C. Development of an equivalent composite honeycomb model: a finite element study. *Applied Composite Materials*. 2016;23(6):1177-94.
155. Gornet L, Marckmann G, editors. Failure and effective elastic properties predictions of Nomex (R) honeycomb cores. 12th European Conference on Composite Materials (ECCM 12); 2006.
156. Hohe and Jr, Becker W. Effective stress-strain relations for two-dimensional cellular sandwich cores: Homogenization, material models, and properties. *Appl Mech Rev*. 2002;55(1):61-87.
157. Li K, Gao X-L, Wang J. Dynamic crushing behavior of honeycomb structures with irregular cell shapes and non-uniform cell wall thickness. *International Journal of Solids and Structures*. 2007;44(14-15):5003-26.
158. ASTM D. 828, entitled "Standard Test Method for Tensile Properties of Paper and Paperboard Using Constant-Rate-of-Elongation Apparatus,". *Annual Book of ASTM Standards*, American Society for Testing and Materials. 1997.
159. Standard A. C271. Standard Test Method for Density of Sandwich Core Materials ASTM International: West Conshohocken, PA, USA. 2004.
160. Standard A. C297 (1994). Standard test method for flatwise tensile strength of sandwich constructions. ASTM C297.94.
161. Standard A. C365 (1994). Standard test method for flatwise compressive properties of sandwich cores. ASTM C365.94.
162. ASTM C. 273-00, 2000. Standard test method for shear properties of sandwich core materials ASTM, Philadelphia, PA.
163. Astm C. 393, Standard Test. Method for Flexural Properties of Sandwich Constructions. American Society for Testing and Materials Annual Book of ASTM Standards: West Conshohocken, PA, USA. 2000.
164. Abbadi A, Koutsawa Y, Carmasol A, Belouettar S, Azari Z. Experimental and numerical characterization of honeycomb sandwich composite panels. *Simulation Modelling Practice and Theory*. 2009;17(10):1533-47.

165. Stocchi A, Colabella L, Cisilino A, Álvarez V. Manufacturing and testing of a sandwich panel honeycomb core reinforced with natural-fiber fabrics. *Materials & Design*. 2014;55:394-403.

LIST OF PUBLICATIONS

- 1) MS Khan, SSR Kolor, MN Tamin. Effects of cell aspect ratio and relative density on deformation response and failure of honeycomb core structure. *Materials Research Express*. 2020 Jan 20;7(1):015332.
DOI: 10.1088/2053-1591/ab6926 (ISI Indexed Q3, IF = 1.929)
- 2) MS Khan, A Abdul-Latif, SSR Kolor, M Petru, MN Tamin. Representative cell analysis for damage-based failure model of polymer hexagonal honeycomb structure under the out-of-plane loadings. *Polymers*. 2021 Jan;13(1):52.
DOI: 10.3390/polym13010052 (ISI Indexed Q1, IF = 3.426)